using the high-temperature flux technique is a notable example of another approach.

For ceramic materials, there are many approaches available to a researcher for fabrication, including the simple pellet press, tape casting, screen printing, sputter deposition (especially PZT and ZnO), sol-gel techniques for thin films, pulsed-laser deposition, and the hygrothermal technique [10] for deposition of quality PZT onto titanium.

Key Research Findings

During World War II, the discovery of PZT was a fortuitous and remarkable improvement on the state of the art in piezoelectric materials engineering. Since then, modest improvements in performance of piezoelectric materials have been made, with the discovery of single-crystal high-strain PMN-PT materials [8] an important milestone. In the past few years, however, methods for studying and manipulating the structure of ceramics on the scale of the unit cell and lower—the grain structure, the ferroelectric domains, and the structure of the unit cells themselves—have appeared [5]. These techniques are especially well-suited for improving the quality of piezoelectric materials; a recent potassium-sodium niobate/lithium tantalate/lithium antimonate ceramic has a piezoelectric performance equivalent to PZT while eliminating toxic lead [12]. Further, given the need to fabricate ►thin-film devices with features measured in nanometers in conjunction with micro- and nanofluidics, an understanding of the nature of polarization and ferroelectric domain growth in materials compatible with fabrication at these scales is vital. The applications for this technology span many disciplines: nonvolatile memory for computer technology, sensors and sensors for medical and biological diagnostics and actuators and microwave devices for consumer applications [9].

Future Directions for Research

The development of characterization and fabrication methods approaching the unit-cell size of known piezoelectric materials has reenergized the area of piezoelectric materials research in the past few years. By tailoring the structure of piezoelectric materials to maximize the polarizability, strength, and maximum strain, major advances are just beginning to appear. Work on applying the replete knowledge of bulk piezoelectric materials to thin-film materials research remains incomplete, from fabrication of PMN-PT to lead-free ceramics at small scales.

Looking beyond ceramic materials to electrets, polymer and elastomeric piezoelectric materials, and so-called electroactive materials, a wide-open field of research in high-strain piezoelectric materials is appearing. Using the same technology to manipulate the chemical and physical structures of complex ionic or nanotube-imbibed polymers, strains of well over 50 % have been obtained in this new class of material, many examples of which are biocompatible. Improvements in reliability, tolerance of extreme ambient conditions, and modeling are important areas that remain to be considered.

Cross References

► Piezoelectric Microdispenser

References

1. Auld BA (1989) Acoustic fields and waves in solids, vol. 1. Krieger, Malabar
2. Bellaiche L, Vanderbilt D (1999) Intrinsic piezoelectric response in perovskite alloys: PMN-PT versus PZT. Phys Rev Lett 83(7):1347–1350
3. Dieulesaint E, Royer D (2000) Elastic Waves in Solids II. Springer, Berlin
4. Hearmon RFS (1956) The elastic constants of anisotropic materials II. Adv Phys 5(19):323–382
5. Hong S, Woo J, Shin H, Jeon J, Pak Y, Colla E, Setter N, Kim E, No K (2006) Principle of ferroelectric domain imaging using atomic force microscope. J Appl Phys 89(2):1377–1386
6. Lang SB (1999) History of pyroelectricity: from ancient greece to space missions. Ferroelectrics 230(1):401
7. Leedom D, Krimholtz R, Matthaei G (1971) Equivalent Circuits for Transducers Having Arbitrary Even-Or Odd-Symmetry Piezoelectric Excitation. IEEE Trans Son Ultrason 18(3):128–141
8. Park S, Shrout T (1997) Ultrahigh strain and piezoelectric behavior in relaxor based ferroelectric single crystals. J Appl Phys 82:1804
9. Setter N, Damjanovic D, Eng L, Fox G, Gevorgian S, Hong S, Kingon A, Kohlstedt H, Park N, Stephenson G et al (2006) Ferroelectric thin films: Review of materials, properties, and applications. J Appl Phys 100(5):51606–51606
10. Shimomura K, Tsurumi T, Ohba Y, Daimon M (1991) Preparation of lead zirconate titanate thin film by hydrothermal method. Jpn J Appl Phys 30(9B):2174–2177
11. Smits J (1976) Iterative Method for Accurate Determination of the Real and Imaginary Parts of the Materials Coefficients of Piezoelectric Ceramics. IEEE Trans Son Ultrason 23(6):393–401
12. Takao H, Tani T, Nonoyama T, Takatori K, Homma T, Nagaya T, Nakamura M (2004) Lead-free piezoceramics. Nature 432:84–87
13. Tiersten HF (1967) Hamilton's principle for linear piezoelectric media. Proc IEEE 55(8):1523–1524
14. Warner AW, Berlincourt D, Meitzler AH, Tiersten HF, Coquin GA, Welsh IFS (1988) IEEE standard on piezoelectricity (ANSI/IEEE standard 176-1987). Technical report, The Institute of Electrical and Electronics Engineers, Inc.

Piezoelectric Microdispenser

JAMES FRIEND, LESLIE YEO
james.friend@eng.monash.edu.au,
leslie.yeo@eng.monash.edu.au

Synonyms

Piezoelectric ink jet; Piezoelectric drop-on-demand; Droplet generator; Piezoelectric micro/nanoliter droplet dispenser

Definition

A fluid-filled chamber that has one or more exit orifices (nozzles) through which the fluid is driven by piezoelectric material causing either a rapid increase in pressure within the fluid or an acceleration of the orifice with respect to the fluid body. Additional fluid is provided through an inlet orifice by external pressure or through a suction mechanism designed into the microdispenser. The fluid, once forced through the nozzles, forms one or more droplets through an instability mechanism – main and perhaps ►satellite droplets – that propagate away from the nozzle, usually at a speed several times the diameter of the droplet per second at speeds up to 10 m/s. The droplets characteristically have a diameter of the same order as the nozzle diameter, usually 1 to 100 μm, and have a volume of several picoliters to nanoliters as they form over a period of about 100 μs. To deliver the fluidic pressure wave required to form the droplets, a pulse or tailored electric drive signal must be provided to the piezoelectric material at a voltage of 5 to 200 V.

Overview

The ►piezoelectric microdispenser, closely related to ►piezoelectric ink-jet printing, a specific application of the microdispenser traditionally for consumer printing, encompasses three separate operating schemes depending on the intended application. A single ►droplet on demand may be delivered by a dispenser through either impulse excitation of the piezoelectric element or continuous vibration of the nozzle with short-term contact onto an application surface. Continuous droplet generation may be obtained through formation of a long-term Rayleigh instability of the fluid surface at the nozzle. ►Fluid jetting is another method to form fibers or droplets, the latter through subsequent breakup of the jet after it has left the microdispenser's exit nozzle due to Rayleigh or Kelvin–Hemholtz instabilities. Another less common method, ►free-surface atomization, makes use of sessile droplets or relatively large fluid volumes placed on the surface of an ultrasonically vibrating structure which induces breakup through an as-yet poorly understood combination of Rayleigh instability and ►cavitation mechanisms.

Piezoelectric microdispensers have existed since the 1950's, though their use increased dramatically with a need for inexpensive printing from the early 1980's, an application shared with thermoelectric (bubble) microdispensers. Generally, piezoelectric microdispensers offer superior flexibility, simplicity, and scalability compared to other known droplet-forming technologies. However, the use of piezoelectric materials causes problems, particularly in the use of lead zirconate titanate (PZT) and its higher-performance doped variants, which are not generally compatible with standard micromachining processes. As a consequence, scaling down dispensers that make use of PZT is difficult. Though other piezoelectric materials have been used over the years, including quartz, aluminum nitride, and zinc oxide, PZT is favored for its large ►electromechanical coupling and relatively large ►piezoelectric strain coefficients. The generation of a sufficient electric field in the piezoelectric materials, particularly for pulsed drop-on-demand dispensers, can require high voltages not directly compatible with integrated-circuit voltages (5 or 12 V). The placement, diameter, and configuration of the inlet and outlet orifices is critical to obtain suitable droplet formation from input strain pulses along the boundary of the fluid chamber, and microdispenser design is a challenge met through a combination of approximate analytical methods, computational modeling, and experimental development, using many versions of a design to discover the one most suitable for the application. Over the years, different operating schemes have been considered for piezoelectric microdispensers, and current technology [1] is essentially a refinement of the spectrum of configurations available over 25 years ago [2].

Regardless, a majority of the systems operate through direct squeezing of the fluid volume present within the dispenser, and as a consequence the volume of fluid ejected from the dispenser at the nozzle is a linear function of the applied voltage, that is, once the stability of the fluid ►meniscus present across the nozzle is overcome. This is in contrast to the generation of jets and droplets via ►acoustic streaming, which would result in an ejected fluid volume proportional to the square of the applied voltage. Applying low voltage signals to the piezoelectric element will result in a deformation of the meniscus, and as the applied voltage is increased, the deformation grows until the meniscus becomes unstable.

If the capillary wavelength is approximately the same size or larger than the nozzle diameter, the formed droplet diameter will be related to the nozzle diameter, and will increase with an increase in the applied voltage. At a certain threshold voltage, more than one droplet will form from the extension and breakaway of the meniscus. Typically, each of the extra droplets – a ►satellite drop – is smaller in size than the primary droplet, but as the voltage continues to increase, these droplets tend to increase in number and volume. There may be yet another transi-

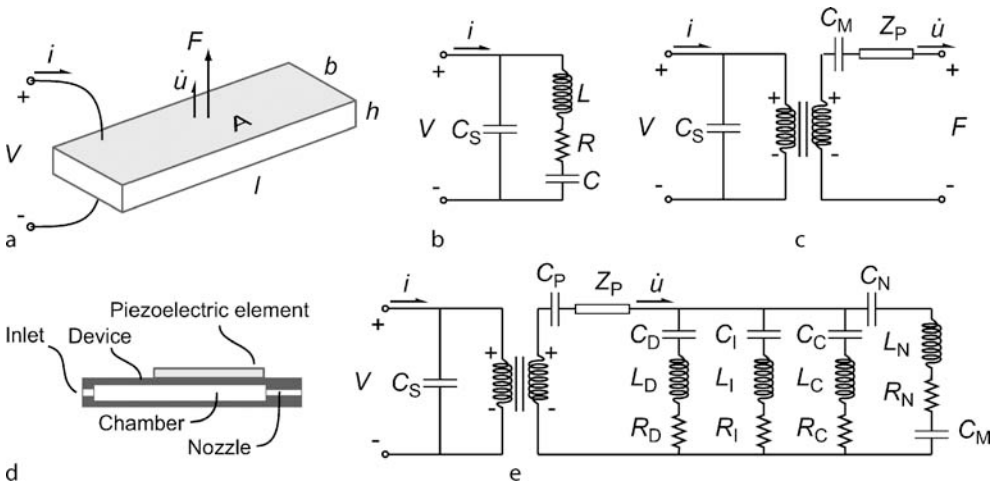

Piezoelectric Microdispenser, Figure 1 Equivalent circuit modeling of (**a**) planar, thickness-polarized, thickness-vibrating piezoelectric transducers using (**b**) a simple lumped-element Van Dyke model and (**c**) a more complex transmission-line model. A model of a piezoelectric microdispenser (**d**) may be formed by connecting the output terminals to the equivalent circuit model of the remaining components (**e**)

tion to chaotic droplet and stream generation as the voltage continues to increase, and cavitation within the chamber or at the nozzle may also occur.

However, if the capillary wavelength is much less than the diameter of the nozzle, the droplet diameter will instead be related to the capillary wavelength: the droplets form from crest instabilities on the free surface of the fluid. The droplet dimensions for this arrangement follow similar trends as the voltage is increased. Using this technique, it is possible to generate droplets less than 1 μm in diameter through the use of frequencies beyond 10 MHz generated from ► surface acoustic wave devices.

This review considers the variety of device designs for piezoelectric microdispensers, methods to model their overall behavior, in addition to the characteristics of atomization mechanisms available for dispensing droplets using piezoelectric materials.

Basic Methodology

Device modeling

Equivalent circuit models have been used to represent piezoelectric material behavior for many years, but are not without limitations. The most common representation for a piezoelectric material, as recommended by the IRE/IEEE standards on piezoelectricity, is the Van Dyke model as described in detail in ► piezoelectric materials in microfluidics, with a capacitor, resistor, and inductor in series representing a single resonance, or motional component of the piezoelectric element, all set in parallel with a second capacitor, representing the ► shunt capacitance. Additional resonances may be included by placing additional capacitor-resistor-inductor sets in parallel, but therein lies some of the limitations of equivalent circuit modeling: accurate determination of the equivalent circuit components requires either a physical prototype or an accurate computational model to provide the data. Further, assuming the loss mechanisms are isolated to a single resistance in the motional component per resonance may lead to error in predicting both the system response and the resonance frequencies. Computational models using finite-element analysis or the like require similar physical data, and so a physical prototype becomes absolutely necessary in the prediction of microdispenser behavior.

Additional matters to consider in using piezoelectric materials that require a physical prototype include the aging of the piezoelectric material and the temperature change during operation. Over time, the resonance frequency and static capacitance will change in an exponential fashion; most of the aging will occur in the first two months, but the subsequent aging can be important in circuit and resonant chamber design. As an electric field is applied to a piezoelectric element, the element will heat due to electromechanical losses in the material. The heating can be significant for soft piezoelectric materials, and can affect the resonance frequencies and capacitance for both hard and soft piezoelectric media.

Equivalent circuit modeling is a useful and commonly applied analysis approach for designing piezoelectric microdispenser systems. The method has limited accuracy, and the ► lumped analysis approach requires the wavelength of the input signal to be larger than any characteristic length within the device. In a microdispenser with an internal cavity, for example, the ► Hemholtz resonance

of the orifice, nozzle, and cavity structure should be far higher than the frequency of excitation of the device used to perform the dispensing. The time required to transmit a change in the applied electric field on the piezoelectric element to a change in the meniscus shape at the nozzle is therefore negligible. Using ▶ transmission-line models of the piezoelectric element, fluid chamber, and other components in the microdispenser permit analysis without the wavelength limitation [3], and provide the ability to analyze the approximate interaction between multiple resonances in the complete system.

In this situation the coupling coefficient of the piezoelectric material is especially important. Though there are many specific forms of the coupling coefficient, an effective coupling coefficient may be used for a transducer operating near a particular resonance;

$$k_{\text{eff}} = \sqrt{\frac{\text{mechanical energy stored}}{\text{electrical energy input}}} = \sqrt{1 - \frac{f_r^2}{f_a^2}}$$

where f_r is the resonance frequency and f_a is the antiresonance frequency (▶ resonance and antiresonance frequency) associated with the vibration mode that dominates the motion induced by the applied voltage signal, if one such mode can be assumed to exist. The mechanical energy stored in the piezoelectric device may then be used to perform work on the fluid meniscus, and in this way the amount of energy applied to form a droplet for a microdispenser as a fraction of the input electrical energy may be estimated once one knows the resonance and antiresonance frequencies. The resonance and antiresonance frequencies are typically near the frequencies of minimum and maximum impedance, respectively, for a specific resonance.

Choosing a thickness-polarized, thickness-vibrating piezoelectric element as an example, we can define the applied voltage V, current i, dimensions b, h, and l, and the output force and velocity F and $\dot{u}$; the cross-sectional area bounded by b and l can be defined by A; here it is assumed this area is electroded on the top and bottom faces of the element and that b and l are much greater than h. Treating it as a collection of discrete circuit elements as shown in Fig. 1b, the Van Dyke circuit, allows the analysis of one resonance within the isolated element. Most piezoelectric materials are capacitive insulators, and the ▶ shunt capacitance $C_S = bl/\beta_{33}^S h$ is the constant capacitance present across the element. The additional branch in the circuit represents the specific resonance being analyzed, the motional branch with inductance L, resistance R, and capacitance C. Many impedance analyzers provide this circuit as a means to model the electrical behavior of the piezoelectric element. The coupling coefficient for this specific arrangement is $k_T = \sqrt{h_{33}^S \varepsilon_{33}^S / c_{33}^S}$. Unfortunately, the model only accounts for one resonance and provides no information on the output force F and velocity $\dot{u}$. By treating the element as a transmission-line impedance Z_P as shown in Fig. 1c, one can incorporate an arbitrary number of resonances, where $C_M = -h_{33}^S bl/\beta_{33}^S h$ and $Z_P = \frac{k}{j\omega} \frac{\omega h/c}{\tan(\omega h/c)}$ where $c = \sqrt{c_{33}^D/\rho}$ is the longitudinal wave velocity for an open-circuit element. The resonances appear when $(\tan \omega h/c)$ goes to infinity. The quantities h_{33}, β_{33}, e_{33}, and c_{33} represent the piezoelectric field to strain coupling, permittivity, inverse permittivity, and material stiffness along the thickness direction in this model. The S superscript on these quantities represents constant strain (clamped) values, and the D represents constant electric field displacement (open-circuit) values. By connecting the output of the piezoelectric element, or port, to a microfluidics structure (see Fig. 1d) with nozzle, chamber, inlet and compliant structure, a microdispenser can be formed. A simple representation of this situation can be modeled as a collection of RLC resistance-induction-capacitance branches in Fig. 1e connected to the output of the piezoelectric element represented by the open terminals on the right in Fig. 1c. Note the inclusion of RLC sets for the device, inlet, device, and nozzle, each treating a specific resonance of the component. Transmission-line impedances could be used for these components as well to handle multiple resonances. There is an additional capacitor for the meniscus to take into account the formation of capillary waves; the charging of the capacitor is tied to the appearance of the capillary waves and can suggest whether a droplet will be formed as a consequence of an input signal V. The values of the resistance, inductance and capacitance may be related back to the dimensions and configuration of the microdispenser as shown by Berger and Recktenwald [3].

Generation

Modeling of piezoelectric microdispensers provides useful information on the potential for further optimization and insights into the operating mechanism underlying their behavior. However, the reliable formation of stable, monodisperse droplets from a device generally requires a tedious process of trial-and-error design of the driving scheme, fluid, nozzle, chamber, and inlet. Many factors affect the behavior of microdispensers, only a few of which can be incorporated into a mathematical model of the overall device at present. Most of the difficulty is associated with the behavior of the fluid at the exit nozzle. Generally, if the fluid to be dispensed has a low viscosity of about 1 – 50 cS, is slightly hydrophobic, and does

not contain particles greater than 10% of the diameter of the nozzle, droplet generation becomes a function of the design of the microdispenser alone [4].

The generation of droplets can be divided into three schemes depending on the form of the fluid leaving the orifice. Individual droplets may be formed on demand through discrete signals applied to the microdispenser, droplets may be formed continuously, with a short transition to and from steady droplet formation upon the application and removal of the driving signal from the microdispenser, or jets of fluid can be generated from a microdispenser, which may later break up into droplets as the jet interacts with the environment. A comparison of a characteristic length of the fluid leaving the microdispenser with the nozzle meniscus size provides another way to categorize the generation mechanism of a device. If the characteristic length – droplet diameter, for example – and the meniscus diameter are similar, the characteristic length is typically controlled by the meniscus size. If, however, the characteristic length is significantly smaller than the meniscus size, the characteristic length is controlled instead by the instability mechanism that generated it.

Droplets from Nozzles

Piezoelectric microdispensers that generate droplets of a size defined by the nozzle diameter function either through the interaction of a pressure wave induced in the fluid with the meniscus located at the nozzle, or a rapid acceleration of the meniscus. Either way, a column of fluid is pushed from the nozzle into the surrounding atmosphere. If the column reaches a sufficient length before being drawn back into the nozzle after passage of the pressure wave (πd_{noz} as predicted by Rayleigh [5], where d_{noz} is the nozzle diameter), the free surface will become unstable and pinch off, forming at least one droplet; the droplet diameter he predicted as a consequence of this process, $d_{\mathrm{Rayleigh}} = 1.89 d_{\mathrm{noz}}$, represents an upper bound for the actual droplet diameter. This instability mechanism is not the free-surface Rayleigh instability as commonly understood and described later.

Lee and Lal [6] summarize the work of Lord Rayleigh, Weber, Sterling and many others quite well, and consultation of references in their work provides an introduction to the literature. Rayleigh's result represents the upper bound since it ignores the drag on the column and droplet from the surrounding atmosphere, and subsequent research considered these factors in the analysis. Through the inclusion of a drag model, the droplet size prediction can be made to be more accurate. Consider the column of fluid pushed from the nozzle, and treat the velocity of the column as U, the fluid's density, surface tension, and dynamic viscosity as ρ, σ, and μ, respectively, and the ambient atmosphere's density as $\hat{\rho}$. The ►Weber number of the ambient atmosphere and ►Ohnesorge number of the fluid may then be defined as

$$\hat{\mathrm{We}} = \frac{\hat{\rho} U^2 d_{\mathrm{noz}}}{\sigma} \tag{1}$$

$$\text{and } \mathrm{Z} = \frac{\mu}{\sqrt{\rho \sigma d_{\mathrm{noz}}}}. \tag{2}$$

Typically, the Weber and Ohnesorge numbers are dimensionless measures of the relative strength of the inertia to the surface tension in a fluid, and the viscosity to the surface tension of a fluid, respectively. Here the Weber number is modified (with a hat, $\hat{\mathrm{We}}$) to consider the inertia of the surrounding atmosphere in comparison to the surface tension of the fluid extending from the nozzle.

As the fluid column extends from the nozzle, the instability of the free surface is exhibited across several length scales, represented by a collection of solutions of Sterling's equation of motion describing the instability. One of these solutions grows in amplitude more rapidly than the others, which caused Sterling to assume that it would come to dominate the droplet formation process. The selected solution describes the maximum column length that can be obtained without actually causing sufficient surface instability to form a droplet. It further describes the diameter of the droplet formed as a consequence of the instability once the fluid column surpasses that maximum length. The wavelength of the instability as it forms a droplet may be written as $\lambda = \pi d_{\mathrm{noz}} \hat{\vartheta}$, where

$$\hat{\vartheta} = \sqrt{2(1 + 3\mathrm{Z})}\, \mathrm{e}^{-0.035 \hat{\mathrm{We}}} \tag{3}$$

represents the reciprocal non-dimensional wavenumber of the most rapidly growing disturbance. For water being ejected from a 10 μm diameter nozzle at $U = 1\,\mathrm{m/s}$, the modified Weber number is $\hat{\mathrm{We}} = 1.81 \times 10^{-4}$, the Ohnesorge number is $\mathrm{Z} = 0.0373$, and so $\hat{\vartheta} = 1.49$ and the wavelength of the instability is $\lambda = 46.9\,\mu\mathrm{m}$. The diameter of the droplet may be taken as one-half the instability wavelength, $d = 23.4\,\mu\mathrm{m}$, because one-half of the wavelength forms the droplet while the other half forms the neck region that separates the droplet from the remaining portion of the fluid column. The fluid's density, surface tension, and dynamic viscosity were treated as $\rho = 1002\,\mathrm{kg/m^3}$, $\sigma = 0.072\,\mathrm{N/m}$, and $\mu = 1.002 \times 10^{-3}\,\mathrm{kg/(m-s)}$, respectively, and the ambient atmosphere's density was set at $\hat{\rho} = 1.3\,\mathrm{kg/m^3}$.

The formation of additional droplets – ►satellite droplets – in addition to the desired or primary droplet for each

extension of the fluid column induced by an applied pressure wave or acceleration of the nozzle is a troublesome problem with microdispensers. Dong, et al., in a thorough work [7], examined the formation of the primary and satellite droplets and suggested a criteria for avoiding the formation of satellite droplets. As the primary droplet forms from the liquid column extending from the nozzle, a fluid thread may form from the neck. In some cases, this fluid thread may become quite long in comparison to the nozzle diameter, the ratio of which could be defined as l_b/d_{noz}. If the fluid thread length is larger than a limiting value l_b^*, the thread will break up into satellite droplets. There is the possibility that the satellite droplets will merge with the primary droplet if the relative velocities are in the correct direction and large enough to induce recombination.

In any case, the limiting value of the fluid thread length may be written as

$$l_b^* = d_{noz}\left(\frac{(C_2 - C_1)a}{2\alpha_{max}^*} + 1\right), \tag{4}$$

where

$$\alpha_{max}^* = \sqrt{\frac{2\vartheta^2 - 2 + 9Z^2}{4\vartheta^4}} \tag{5}$$

is a term related solely to the nozzle and fluid characteristics; $\vartheta = \sqrt{2(1+3Z)}$ here, an approximation similar to Dong, et al., in line with Sterling's analysis given by Eq. (3) with the omission of the Weber-related air drag term. The nondimensional constants C_1 and C_2 are related to the pinch-off time of the liquid thread from the nozzle and primary droplet, respectively, while a represents another nondimensional constant that relates the speed of the wave disturbance along the periphery of the fluid column to the speed of the retreating fluid column back towards the nozzle after the formation of the droplet and fluid thread stretching between the column and droplet. Dong, et al., claim the product $(C_2 - C_1)a$ is between 0.9 and 1.1 for their experiments with water and glycerin compounds ejected into air. For the water/air system considered in this section, the limiting fluid thread length is $l_b^* = 22.8\,\mu m$ if $(C_2 - C_1)a$ is 0.9. Experimental visualization would be necessary to determine the actual fluid thread length. Dong, et al., suggest that the most effective method to eliminate satellite droplet formation is an increase in the fluid viscosity which would increase the Ohnesorge number and reduce α_{max}^*.

Most piezoelectric microdispensers use the single-droplet nozzle ejection mechanism to form droplets. Through careful design, droplets may be rapidly ejected one after another from the meniscus at frequencies of up to 10 kHz, though there are limitations from refill speed, cavitation, bubble ingestion from the nozzle into the fluid chamber, and satellite droplet formation. Generally the piezoelectric material is not a limitation in droplet delivery speed unless soft PZT is used, which has a larger electromechanical transduction loss and is susceptible to heating at operating frequencies above 1 kHz.

Jetting from nozzles in piezoelectric microdispensers is also possible, usually through a combination of constant applied pressure on the fluid with a lesser modulation of the pressure using the piezoelectric element. The modulation introduces an instability in the jet traveling out of the orifice which is amplified to cause the breakup of the jet into droplets through the interaction of the jet with the ambient environment; this instability mechanism is known as the ▶ Kelvin–Helmholtz instability and requires the jet to be moving at several meters per second in air to cause droplet formation [8]. Secondary breakup of the droplets into finer droplets may then occur via the Rayleigh–Taylor mechanism described later, though the conditions under which this can happen do not typically occur on the scales of most piezoelectric microdispensers.

Droplets from Free Surfaces

It is also possible to dispense microdroplets from free surfaces, either formed on a sessile droplet or along the meniscus formed at a nozzle. In the latter case, the critical difference with the previous section is that the primary droplet formed from the nozzle is much smaller than the diameter of the nozzle, eliminating the direct influence of the nozzle's size on the size of the droplet. The study of the formation of droplets from free surfaces has a long and controversial history, which has been suggested to be due to either capillary wave breakup, cavitation, cavitation-induced capillary waves which subsequently break up to form droplets, or even cavitation-screened capillary wave breakup, where a cavitation layer beneath the surface acts to suppress atomization. It is likely that over the wide range of operating frequencies and configurations available each of these physical mechanisms is possible, but for microdispensing fluids, capillary wave breakup appears to be the most likely mechanism [9]. Even so, the complexity of the analysis and nonlinear behavior [10] should not be underestimated in considering the use of free surfaces.

In 1950 Taylor studied the formation of sinusoidal waves on the free surface of a fluid in air undergoing acceleration perpendicular to the free surface and in the direction of the force of gravity, and almost a century prior Rayleigh considered the formation of similar waves if the denser fluid was placed above the free surface; both illus-

trate a similar mechanism that has come to be described by the Rayleigh–Taylor instability. Curiously, the instability will appear between the interfaces of other phases of media, including even solid-solid interfaces, and the form of the equations that describe the instability will remain essentially the same [11]. The formation of droplets from capillary waves may be described by the Rayleigh–Taylor instability.

Loosely following Piriz, et al. [11], if $\xi = \xi(x, t)$ represents the transverse displacement of the inviscid fluid surface where x is the position coordinate along the fluid interface[1], $\ddot{\xi} = A_T \kappa g \xi$ is the equation of motion of the surface if we ignore surface tension and let the ▶ Atwood number be $A_T = \rho_2 - \rho_1/\rho_2 + \rho_1$, $\rho_2 > \rho_1$, where ρ_2 is the density of the fluid above the interface, and g and κ be the gravitational acceleration (9.8065 m/s^2) and the perturbation wave number, respectively. This can be integrated to give the exponential growth of the interface amplitude at a rate of $\sqrt{A_T \kappa g}$. The wavenumber is related here to the frequency of the applied oscillation through $\kappa = f/c$, where f is the frequency of the applied oscillation and c is the bulk sound speed within the fluid carrying the acoustic energy to the interface. If we place the dense fluid beneath the interface so that now ρ_2 is the density of the fluid below the interface, and incorporate surface tension, dynamic viscosity, and the acceleration of the fluid interface $\ddot{\psi}(t)$ in the direction of the gravity force g, the equation of the transverse displacement of the surface $\xi(t)$ becomes

$$\ddot{\xi} + \left[A_T \kappa \left(g - \ddot{\psi}(t)\right) + \sigma/\rho_1\right]\xi + 2\frac{\mu_1 + \mu_2}{\rho_1 + \rho_2}\rho_2 \kappa^2 \dot{\xi} = 0. \tag{6}$$

Lamb recognized in 1932 that the surface tension acts to stabilize disturbances with wavenumbers greater than the cutoff value of

$$\kappa_C = \sqrt{\frac{g(\rho_1 + \rho_2)}{\sigma}}.$$

Above this value, oscillations induced on the free surface are stable, while below this value, it is possible to induce instability on the surface and form droplets. Viscosity cannot prevent the instability, but it does increase the acceleration $\ddot{\psi}(t)$ necessary to cause the instability to appear. In the equation of motion (6), acceleration due to gravity, g, also acts to stabilize the interface. There are different ways to destabilize the surface, the simplest of which is to $\ddot{\psi}(t)$ to a constant value above $g + \sigma/(\rho_1 A_T \kappa)$, forming a gravity wave. Other ways include harmonic excitation with $\ddot{\psi}(t) = \Psi e^{i2\pi Ft}$ where $i = \sqrt{-1}$, Ψ is the amplitude, and F is the frequency of excitation. Lang [9] found the diameter of the droplets formed from the free surface closely follows Kelvin's equation for the capillary wavelength,

$$\lambda = \sqrt[3]{\frac{2\pi\sigma}{\rho f^2}}, \tag{7}$$

where f represents the frequency of the most easily excited capillary waves on the free surface. Based on experimental results, it has been shown that the frequency of the capillary waves is one-half the excitation frequency F if it is assumed to be harmonic, and Lang showed that the droplet diameter is 0.34 times the capillary wavelength based on experimental results across a wide range of frequencies:

$$d = 0.34\sqrt[3]{\frac{8\pi\sigma}{\rho f^2}}.$$

Similar to the droplet breakup model in the previous section, many different vibration modes may be excited on the surface by the acceleration $\ddot{\psi}(t)$, but the one represented by λ in equation is assumed to dominate in the generation of droplets. This assumption is valid at powers just sufficient to cause the generation of droplets, but as the amplitude Ψ is further increased, other modes may become large enough to form droplets, increasing the droplet size distribution and the complexity of analysis.

Impulsive excitation may also be used to form droplets from a free surface in this way. Continuous wave excitation can provide very monodisperse distributions of droplets with diameters much less than the characteristic size of the free surface [12], but impulsive excitation has also been used with success in commercial applications by Xerox [4]. A critical part of their success has been in finding ways to form a single droplet from the surface per excitation pulse; typical free surface droplet generators form n droplets where $n = (1/2)\pi(d_{surf}/\lambda)^2$, d_{surf} is the diameter of the free surface, and λ is the capillary wavelength. Impulsive excitation has the advantage of offering droplet-on-demand operation at the expense of requiring thorough analysis of the free surface to ensure reliable formation of individual droplets.

Jetting from the free surface may also be obtained, and droplets could be formed from these jets through secondary breakup mechanisms if the Ohsenorge number is less than about 0.1 and the Weber number is above 5. The conditions necessary to obtain free-surface jetting from piezoelectric microdispensers are fairly challenging; even though there are examples of high-frequency free-surface

[1] A 2-D assumption is implicit here, as it is throughout most literature on instability calculations.

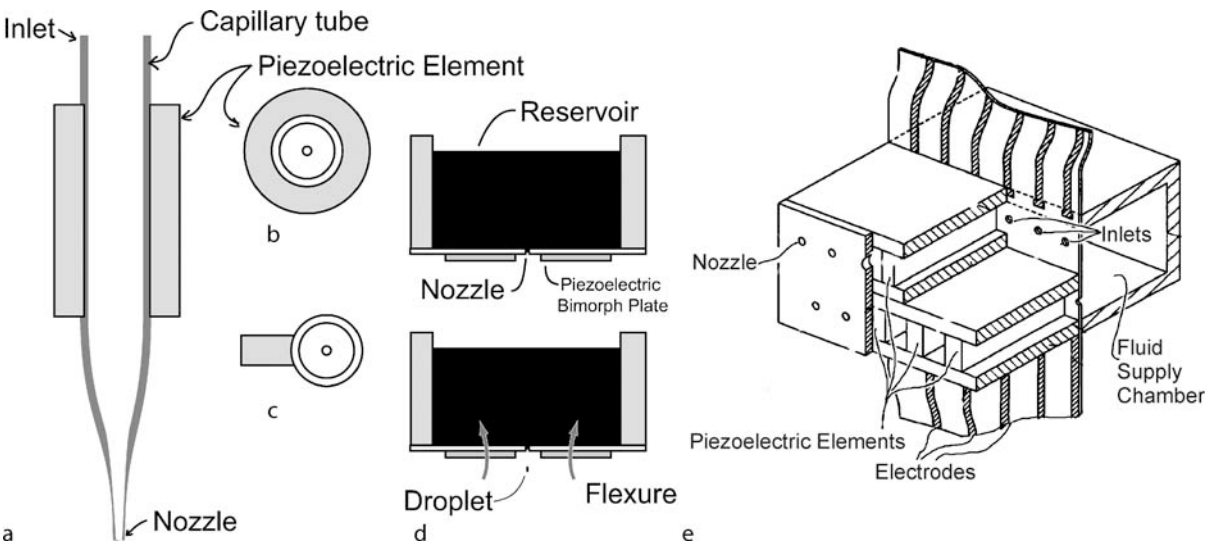

Piezoelectric Microdispenser, Figure 2 The capillary tube microdispenser, viewed from the side (**a**) and top (**b**), with a variation (**c**) by Lee and Lal [6]. Though almost unrecognizable after years of refinement and adoption of a parallel layout scheme, the Konica-Minolta device (**d**) is also a capillary tube microdispenser

jetting [13], they at present remain little more than curiosities.

Droplet Motion After Ejection

Once formed, most piezoelectrically-dispensed droplets have a drag force proportional to their velocity. In contrast to the viscous drag force on macroscopic objects,

$$F_{\text{Viscous Drag}} = \tfrac{1}{2}\rho C_{\text{d}} A v^2 , \tag{8}$$

which scales with the square of the velocity of the object relative to the surrounding fluid, the drag force due to Stokes' law scales linearly with velocity:

$$F_{\text{Stokes}} = 6\pi\eta r v ; \tag{9}$$

$r, v, A, C_{\text{d}}, \rho$, and η are the drop's radius, velocity, and cross-sectional area, the coefficient of drag, and the surrounding fluid's density and viscosity, respectively. The viscous drag scales inversely to the square of the diameter of the droplet, and so is negligible in air for droplets less than about 25 μm in diameter. The most common figure of merit used in choosing the appropriate drag force is the ▶ Reynolds number.

For droplets in air less than about 5 μm in diameter, the actual drag force is even lower, since the surrounding air is not a continuum at these scales. Millikan's resistance factor (or ▶ Cunningham's correction) multiplies the terms on the right-hand side of equation (9) to form the corrected drag force

$$F'_{\text{Stokes}} = 6\pi\eta r v \left[1 + \left(\frac{0.130\,\mu\text{m}}{d}\right) \times \left(1.252 + 0.399\,\text{e}^{-1.100 d/0.130\mu\text{m}}\right)\right] \tag{10}$$

A 10 μm diameter droplet moving at 1 m/s in air would have 14.1 pN, 1.72 nN, and 2.00 nN of force on it from viscous drag, uncorrected Stokes' drag, and Cunningham-corrected Stokes' drag, respectively. More importantly, the deceleration of a 10 μm diameter water droplet moving at 1 m/s would be 3820 m/s^2 due to the Cunningham-corrected Stokes drag calculated from

$$\dot{v} = \text{F}'_{\text{Stokes}} \Big/ \left(\frac{\pi}{6}\rho d^3\right) \tag{11}$$

where the term in parentheses is the droplet mass. The deceleration decreases rapidly as the droplet slows; the velocity is an exponential function of time. Under gravity, the terminal velocity can be found by setting the drag force equal to the force of gravity, though this is far less than the ejection velocities for most dispenser systems; for example, a 10 μm droplet has a terminal velocity of only 3 mm/s.

In addition to the correction on the drag force from the noncontiguous surrounding fluid, there is also an randomizing effect on the droplets' motion due to the interaction with the environment: ▶ Brownian motion. This motion can cause error in droplet placement or

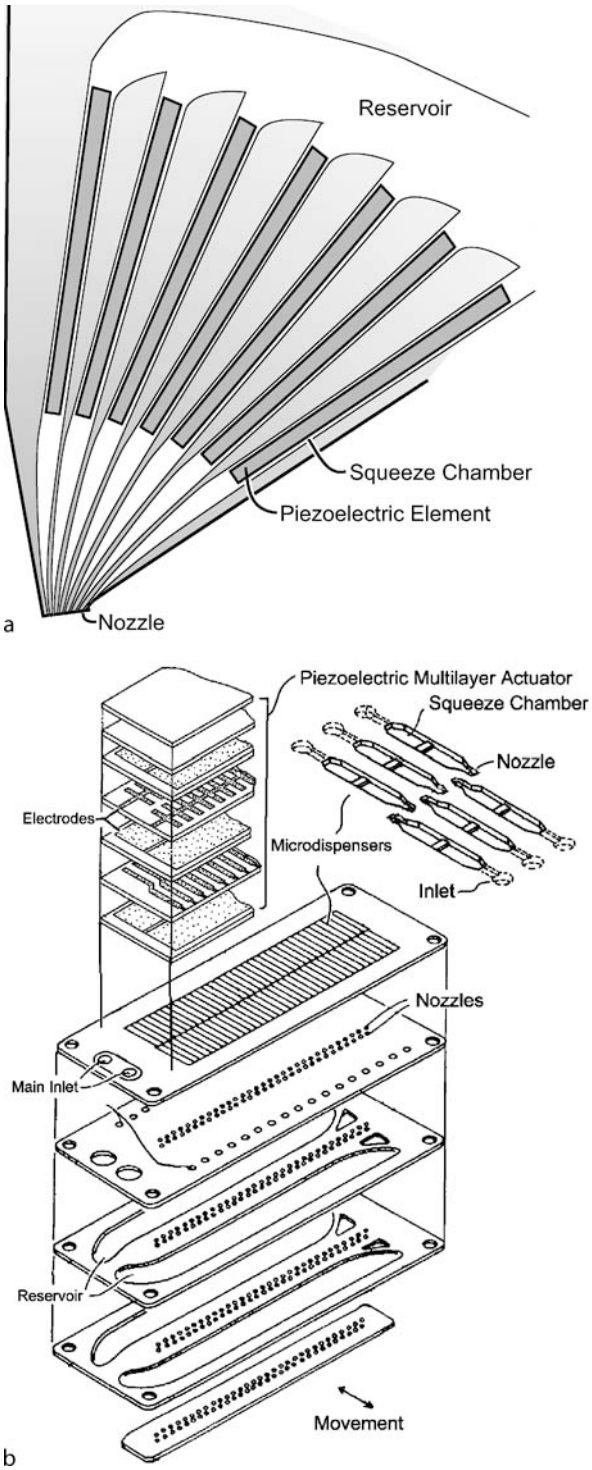

Piezoelectric Microdispenser, Figure 3 The side-shooter design as conceived by Kyser and his associates at Silonics in the 1970's (**a**), and a modern version by Brother (**b**) using planar micromachining technology. Note the dramatic increase in nozzles and the more detailed cross-sectional design. The chamber cross-section in the Kyser design is rectangular

agglomeration of droplets in continuous droplet formation or atomization systems. The mean displacement of a droplet, δ, due to Brownian interaction over time t is a function of the temperature T, ▶ Boltzmann's constant $k = 1.38065 \times 10^{-23}$ J/K, and drag force, F_{Drag}, which is a choice between Eqs. (8) through (10) suited to the diameter of the droplet under consideration,

$$\delta = \sqrt{\frac{2kTt}{F_{\text{Drag}}}}. \tag{12}$$

For a 5 μm droplet, the average displacement after one second at 20 °C is about 2.66 μm, over half the droplet's radius, using Eq. (10) for the drag force.

Key Research Findings

The devices resulting from the combination of piezoelectric materials and fluidic microstructures to provide dispensing of small amounts of liquid fall into several distinct categories based on their construction. Most common of these is the capillary tube drop-on-demand system, shown in Fig. 2, first developed by Zoltan at Clevite in the early 1970's, and commonly called the Gould or Bogy device. Many variations on this design exist due to the simplicity of the configuration and ease in forming the micropipette tips from which droplets may be dispensed; one can even manufacture their own capillary tube microdispenser for very little cost [4]. Fig. 2a illustrates the typical form of this device, though there have been many variations in the shape of the piezoelectric element used, as shown with the top views in Fig. 2b and c; the latter from Lee and Lal [6], and an interesting variation (see Fig. 2d) from Percin and Khuri-Yakub [14]. Through mass production and microfabrication techniques, the concept has been refined to the form shown in Fig. 2e by Konica-Minolta [15]. The device functions either by squeezing the fluid or accelerating the meniscus through actuation of the piezoelectric material; in most devices both mechanisms are in part responsible for the ejection of droplets. Note even in the Konica-Minolta device the piezoelectric material is a simple shape that may be constructed from machining bulk pieces of PZT. Another design that has been used for microdispensers is the so-called side-shooter design originally developed by Kyser and others in the late 1970's, as illustrated in Fig. 3 in its original configuration, and a modern configuration by Brother making use of planar micromachining technology. A relatively unique version of droplet generation from a free surface is focused acoustic beam ejection by Elrod, et al., at Xerox PARC in the early 1990's [4] illustrated in Fig. 4; it represents a refined version yet lower-frequency ver-

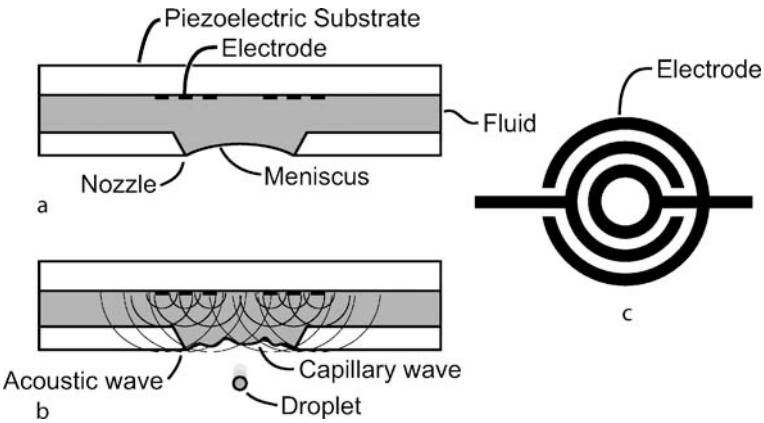

Piezoelectric Microdispenser, Figure 4 Focused acoustic beam ejection technology by Elrod and associates at Xerox PARC. Using a piezoelectric element with electrodes immersed in a thin layer of fluid below a nozzle (**a**), an electrical impulse will induce an acoustic wave that, when interacting with the meniscus, forms a capillary wave that ejects a single droplet (**b**). The form of the electrode (**c**) and the driving signal are two of the features of the design that must be carefully designed

sion of the surface acoustic wave atomizer by Shiokawa et al. [13].

Future Directions for Research

Recently, many new piezoelectric materials have appeared as a consequence of the ability to observe and tailor crystal, polycrystalline, and polymer structures on the nanoscale. Indeed the evolution of high-performance piezoelectric materials like PMN-PT, polypyrrole, IPMC, and other electroactive polymers promise to usher in a new generation of materials that offer advantages over PZT for dispensing applications. Meanwhile, compatibility problems in the fabrication of silicon, PZT, and other standard micromachining materials are being solved, offering the ability to apply PZT in ways not currently possible.

In analysis, most microdispensing work assumes the working fluid is Newtonian, while many fluids that are useful for dispensing in the printing, biomedical and microfabrication industries are strongly non-Newtonian. A return to the fundamentals is in order to revisit the use of these fluids in forming droplets. Improved computational algorithms capable of dealing with the free surfaces and multiple physical phenomena of piezoelectric media, structural deformation, and nonlinear acoustic wave propagation will be central to this effort. As the excitation frequencies and power per unit volume are increased, the incorporation of cavitation models will also be beneficial.

Cross References

- ► Acoustic Streaming
- ► Biosample Preparation Lab-on-a-Chip Devices
- ► Cavitation in Microdomains
- ► Control of Microfluidics
- ► Droplet Based Lab-on-Chip Devices
- ► Droplet Dispensing
- ► Membrane Actuation for Micropumps
- ► Microactuators
- ► Microneedles – Applications & Devices
- ► Supersonic Micro-Nozzles
- ► Piezo/PZT in Microfluidics
- ► Ultrasonic Pumps

P

References

1. Burgold J et al (2005) Evolution and operating experiences with different drop-on-demand systems. Macromol Rapid Commun 26(4):265–280
2. Wehl WR (1989) Ink-jet printing: the present state of the art. CompEuro'89, VLSI and Computer Peripherals. VLSI and Microelectronic Applications in Intelligent Peripherals and their Interconnection Networks, Proceedings 2, p 2
3. Berger SS, Recktenwald G (2003) Development of an Improved Model for Piezo-Electric Driven Ink Jets. In: NIP19: International Conference on Digital Printing Technologies. The Society for Imaging Science and Technology, New Orleans
4. Lee ER (2003) Microdrop Generation. In: Lyshevski SE (ed) Nano- and Microscience, Engineering Technology and Medicine Series. CRC Press, New York, p 252
5. Rayleigh L (1878) On the instability of jets. Proc London Math Soc 10:4–13
6. Lee CH, Lal A (2004) Single microdroplet ejection using an ultrasonic longitudinal mode with a PZT/tapered glass capillary. Ultrasonics, Ferroelectrics and Frequency Control, IEEE Trans 51(11):1514–1522
7. Dong H, Carr WW, Morris JF (2006) An experimental study of drop-on-demand drop formation. Phys Fluids 18(7):072102

8. Tanner FX (2004) Development and Validation of a Cascade Atomization and Drop Breakup Model for High-Velocity Dense Sprays. Atomization Sprays 14(3):211–242
9. Lang RJ (1962) Ultrasonic Atomization of Liquids. J Acoust Soc Am 34:6
10. Shi WT, Goodridge CL, Lathrop DP (1997) Beraking waves: bifurcations leading to a singular wave state. Phys Rev E 56(4):4157–4161
11. Piriz AR et al (2005) Rayleigh-Taylor instability in elastic solids. Phys Rev E 72(056313):1–10
12. Forde G, Friend J, Williamson T (2006) Straightforward biodegradable nanoparticle generation through megahertz-order ultrasonic atomization. Appl Phys Lett 89:064105
13. Shiokawa S et al (1989) Liquid streaming and droplet formation caused by leaky Rayleigh waves. In: IEEE Ultrasonics Symposium. IEEE, Montreal
14. Percin G, Khuri-Yakub BT (2003) Piezoelectric droplet ejector for ink-jet printing of fluids and solid particles. Rev Sci Instrum 74(2):1120–1127
15. Okuno T (2006) Inkjet Print Head and Manufacturing Method Thereof, U.S.P. Office. 2006, Konica Minolta Holdings, Ltd.: United States, US2006/0017778, p 21

Piezoelectric Micro/Nanoliter Droplet Dispenser

► Piezoelectric Microdispenser

Piezoelectric Pumps

► Piezoelectric Valves

Piezoelectric Valves

JAMES FRIEND, LESLIE YEO
MicroNanophysics Research Laboratory, Monash University, Clayton, VIC, Australia
james.friend@eng.monash.edu.au,
leslie.yeo@eng.monash.edu.au

Synonyms

Microvalve; Piezoelectric pumps; No-moving-part valves

Definition

Structures that regulate the flow of fluids using piezoelectric materials, either composed of active regulation through deflection of a structure to block or allow passage of the fluid using electrically-driven piezoelectric elements, or as a piezoelectric pump in combination with mechanical or passive diffuser valves.

Overview

Active piezoelectric valves offer a unique combination of large closing forces – hundreds to thousands of newtons – against fluid loads and small displacements measured in the tens of microns. Such valves may be designed to close or open upon the application of an electric field to the piezoelectric material, and offer flow rates from nearly arbitrarily low amounts to tens of liters per minute for gases, water, and similar fluids [1]. Given the limited strain, 0.1% or less, available from typical high-performance piezoelectric ceramic materials, a majority of the research and development effort has been in amplifying this strain to permit efficient valving action. Flap or cantilever valves seated across an orifice actuated as a piezoelectric ►bimorph or ►unimorph or ball or grooved structures seated against an orifice and moved using a large-displacement ►linear multilayer piezoelectric actuator is typical of this approach.

Passive piezoelectric valves function in an entirely different manner, though they also make use of piezoelectric bimorph or unimorph structures. Forming one side of a small fluid chamber, or ►Helmholtz cavity, the piezoelectric element can excite chamber resonances when driven at appropriate frequencies via an oscillatory electric field, usually from 10 Hz to 100 kHz depending on the device dimensions and fluid. With two or more orifices connecting the chamber to the outside, fluid may be passed into and out of the chamber; by using orifices with different shapes the flow direction may be regulated without requiring a mechanical blockage of the flow [2] or moving parts. Though these configurations are effective as pumps [3], they also can serve as valves for applications where some leakage is tolerable, or where ball or flap valves may be used as passive mechanical restrictions on the orifices to augment the sealing action and improve performance.

Cross References

► Piezoelectric Microdispenser
► Piezoelectric Materials for Microfluidics

References

1. Oh K, Ahn C (2006) A review of microvalves. J Micromech Microeng 16:13–39
2. Izzo I, Accoto D, Menciassi A, Schmitt L, Dario P (2007) Modeling and experimental validation of a piezoelectric micropump with novel no-moving-part valves. Sens Actuators A 133(1):128–140
3. Laser D, Santiago J (2004) A review of micropumps. J Micromech Microeng 14(6):35–64

pL

► Picoliter Flow Calibration